INVESTIGATION ON THE PERFORMANCE OF ABRASIVE WATERJET MACHINING ON ARMOR STEEL

A SYNOPSIS

Submitted by

S. RAMMOHAN

(Reg. No. 201917117)

in partial fulfilment for the award of the degree

of

DOCTOR OF PHILOSOPHY

DEPARTMENT OF AUTOMOBILE ENGINEERING

SCHOOL OF MECHANICAL AERO AUTO AND CIVIL ENGINEERING

KALASALINGAM ACADEMY OF RESEARCH AND EDUCATION

(DEEMED TO BE UNIVERSITY)

ANAND NAGAR, KRISHNANKOIL – 626 126

TAMIL NADU, INDIA

MAY 2023

1. INTRODUCTION

Rolled homogeneous armor (RHA) is often utilised in many armor applications [1]. Because of its great energy-absorbing qualities, RHA steel is primarily utilised to build military equipment such as tanks, howitzers, and other armored combat vehicles [2,3]. RHA steel is used for ballistic protection in military and civil applications because of its high hardness and ultimate tensile strength. The ability to enhance its hardness with good toughness has been critical to its effectiveness in achieving high performance. This steel has maintained its high position due to its low price, dependability, access to manufacturing infrastructure, continuous value such as structural material, and simplicity of fabrication [4,5]. Due to their high hardness and strength, these steels cannot be turned or milled. This research attempted to cut RHA steel using an unconventional machining method called abrasive waterjet machining (AWJM) [6]. Due to the constraint of traditional methods, non-conventional methods are used for material removal.

AWJM is an emerging non-conventional process for hard materials like RHA steels. This is particularly due to the characteristics such as the absence of a heat-affected zone, a high-cutting process, the number of co-proficiencies, and the ability to cut complex shapes, among others. Water and a flow of abrasives arrive from two directions in AWJM and become mixed up, and then flow through the nozzle. The impelling force of water is transferred to abrasives. Consequently, the abrasives' velocity is swiftly increased, and they become efficient in cutting any material. The metal removal process is divided into two zones, referred to as the cutting wear zone and the deformation wear zone [7,8]. Material removal in AWJM includes erosion, microchip development, ploughing, and rubbing [9].

The abrasive striking angle and mechanical characteristics of the target material have been critical to the development of each of these mechanisms. The AWJM is gaining acceptance as a standard cutting tool in industries such as nuclear, oil, foundry, automotive, aerospace, and construction. This method may be used in conjunction with wire electric discharge machining (WEDM), plasma flame, and laser cutting. Compared to plasma and laser machining, the cost of AWJM is typically one-quarter that of wire EDM, and it can cut thicker plates with superior dimensional precision [10,11].

2. LITERATURE SURVEY

Literature survey was done on the armour steel, machining on armour steel, s semi-empirical model, regression, and numerical modeling on AWJM.

Lenihan et al. [12]. exhibits that Armoured Fighting Vehicle (AFV) is a military grade vehicle. The hull specifically designed to resist penetration from enemy weapons. Senthil et al. [13]. introduced that projectile is tested with different oblique angles in armour steel plate. The armour steel proved that good ballistic performance. Banerjee et al. [14]. investigated the behaviour of typical armour steel material under large strains, high strain rates and elevated temperatures needs to be investigated to analyse and reliably predict its response to various types of dynamic loading like impact. Iqbal et al. [15]. studied the constitutive behaviour of 14 Armox 500T steel and armour piercing incendiary projectile (API) material under varying stress state, strain rate and temperature. Singh et al. [16]. showed that hot-rolled high nitrogen steel exhibits better ballistic performance against AK-47 and 14.5 AP projectiles than RHA steels.

Ghiorghe et al. [17] studied the influence of process parameters on the dimensional accuracy of parts manufactured by Ramor 550 and Ramor 400 armored steel, using the wire electrical discharge machining (WEDM). Bobbili et al. [18]. investigated the influence of machining parameters on surface roughness (SR) and material removal rate (MRR) of high strength armor steel using wire cut electrical discharge machining (WEDM). El-Taweel et al. [19]. studied the effect of EDM assisted by magnetic field process parameters on the surface integrity of armoured steel (HV500).

Wang. [20]. Conducted an experimental model for the cut depth based on the Buckingham theorem and dimensional analysis. On alumina ceramics, tests were conducted in a multipass AWJM to determine the effect of various parameters on the depth of cut. Yuan et al. [21]. Investigated the grinding of circular pockets on a titanium alloy using AWJM. The Box-Behnken approach examines the input and output parameters, and it has developed a dimensional analysis to compare the experimental and empirical models for milling depth. The average milling depth variations between experimental and forecasted values was 3.5%. Shanmugam and Masood. [22]. Created a semi-empirical model for predicting the kerf taper and verified it using an average percentage deviation and standard deviation. Singh and

Shukla. [23]. Studied AWJM, where semi-empirical dimensional analysis models had been developed and effectively used to estimate the kerf angle and Ra respectively. Pahuja and Ramulu. [24]. created a semi-empirical model to determine the depth of cut in the AWJM of Ti6Al4V, CFRP, and layered Ti/CFR. Mohankumar et al. [25]. developed using AWJM semi-empirical dimensional analysis-based methods to determine the cutting depth, the angle of the kerf, and the roughness of the surface on MMC.

Kumar et al. [26]. carried out an RSM approach on aluminium/ tungsten carbide composites. The influence of AWJM characteristics and their relationships on responses was investigated using the RSM approach. Thamizhvalavan et al. [27]. conducted machinability studies on hybrid metal matrix composites by changing the process parameters and different abrasive materials with different mesh sizes. The RSM approach was used to examine the process parameters. Singh and Shukla. [28]. investigated the kerf characteristics of Inconel 600 by using the RSM approach. SOD was the most influencing parameter in kerf characteristics tics and Jet water pressure was less significant due to its hardness. Shanmugam et al. [29]. analysed the AWJM machining parameters on the aluminium metal matrix by using RSM Approach to determine the kerf angle and surface roughness. They obtained the optimum kerf taper and surface roughness by lower level in jet traverse speed, jet water pressure, and SOD.

Jianming et al. [30]. have constructed a column of Smoothed Particle Hydrodynamics (SPH) particles to represent the properties of water, and then, some of the particle's characteristics are randomly altered to resemble abrasive particles. Additionally, the average diameter provided by the supports matches with the size of the abrasive particles. Anwar et al. [31]. have constructed an AWJM milling Finite Element Model (FEM) with the care of choosing appropriate abrasive particle shapes, sizes, and velocities. However, the influence of water is neglected. Nyaboro et al. [32]. have examined the CFD-erosion method for determining the contour of the machined surface. Wenjun et al. [33]. have proposed a FEM for the AWJM machining process using the arbitrary Lagrange-Euler approach. The erosion wear caused by high velocity abrasive particle impacts has been studied using finite element analysis, which is also widely used. Lozano Torrubia et al. [34]. have examined the AWJM variations to explore different variability. In order to describe the fluid flow accurately, a meshless Lagrangian particle SPH approach has been developed. As a

result, it is commonly used in the simulations of AWJM milling operations.

3. RESEARCH GAP:

- Currently, the profile cutting in Armor steels are carried out with flame cutting. This process induces a wide HAZ region, poor surface quality and thus requires a secondary operation. However, the Abrasive Waterjet Machining eliminates these draw backs and can produce a minimal distortion on the work material.
- Armor material is work hardening material and requires higher shear energy during machining, it will have profound effect during edge preparation through milling operations.
- Non-conventional (AWJM operation): All these problems can be reduced / eliminated through AWJM and it does not produce any HAZ, Sub surface damages and thermal degradation on the work material.
- Few authors done on machining on Armor steel by using Abrasive waterjet machining but not briefly describe the influence of machining characteristics on Armor steel.

4. OBJECTIVES

- To cut the Armor steel through abrasive water jet machine.
- To investigate the AWJM cutting performance by varying the level of water jet pressures, Jet traverse speed and Standoff Distance on the cutting of armor Steel.
- To analyse the various cutting performance characteristics such as kerf characteristics, material removal rate, and surface roughness.
- To perform the microstructural examination on a cut surface during the AWJM.
- To develop a dimensional analysis and with Buckingham's π-theorem, a semi-empirical model was built using both the experimental data and material property data.
- To examine the prediction output responses in the material removal rate (MRR), surface roughness (Ra), and kerf angle (Ka) for the AWJM of armor steel using regression and semi-empirical models.
- To develop an SPH-DEA-FEM approach for predicting the cutting characteristics of abrasive water jet machining over a range of process

parameters as well as for elucidating the underlying mechanism of kerf generation.

5. METHODOLOGY

The methodology followed in the present research work is shown in the Figure

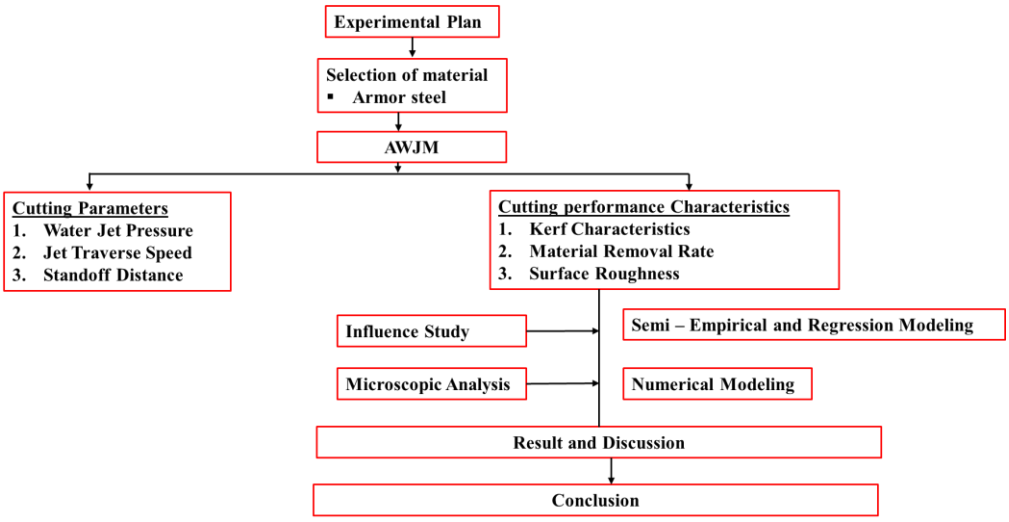

Figure 1 Research Methodology

ORGANIZATION OF THESIS

Chapter 1: This chapter describes the introduction and background of armour steel in armour combat vehicle applications. And it deals with the assessment of conventional and unconventional methods of machining. It also reveals the necessity, applications, merits and demerits of AWJM.

Chapter 2: In this chapter, a thorough literature review about armor steel, machining on armor steel, semi-empirical model, regression, and numerical modeling on AWJM, the research gap, objectives and methodology of the research work are presented.

Chapter 3: This chapter discusses the experimental setup, materials used in this work, selection of AWJ machining parameters, design of experiments and various instruments involved in this work.

The experimental setup used in this work is shown in Figure 2. AWJM trials were carried out on armor steel using M/s. DADRI International makes the DWJ FB-1313 machining centre. Throughout the cutting process, the parameters jet impact angle (90°), garnet abrasive size (80 mesh), nozzle diameter (0.67 mm), and orifice diameter (0.25 mm) were maintained constant. On the basis of the literature and initial

experiments, the AWJM input parameters and their ranges were chosen. AWJM was used to cut a 20 mm straight linear single pass on the armor steel plate. The process parameters were varied at three levels: [Jet pressure = 220, 240, 260 MPa; Jet traverse speed = 5, 10, 15 mm/min; and Standoff distance = 1, 2, 3 mm].

The armor steel material is mainly being used in battlefield tank body structures and various combat applications in the defense industry. The chemical composition of armor steel consisted of various elements, i.e., C, 0.3301%; Mn, 0.563%; Si, 0.1937%; S, 0.0019%; Cr, 1.507%; Ni, 1.570%; Mo, 0.3857%; V, 0.119%; Al, 0.0494; and Fe, balance. The experimental design in this research was based on the L27 factorial design. Work on developing semi-empirical models for considering responses has been expanded in this study. In this study, four quality requirements are chosen that significantly impact the machining of the material using the AWJM technique.

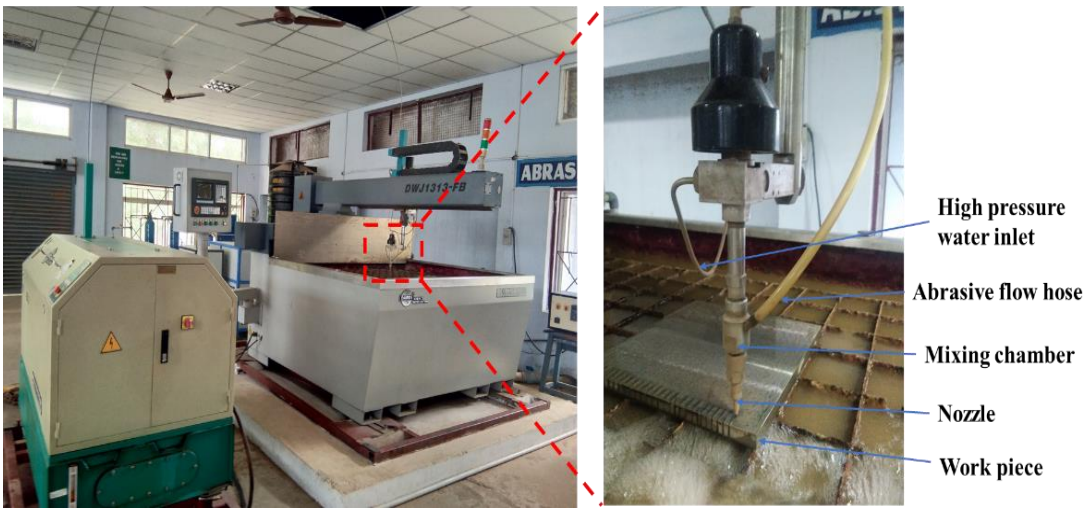

Figure 2. Experimental setup and Close-up view of a workpiece mounted on the machine.

Chapter 4: This chapter discusses the outcomes of AWJM process parameters on surface roughness, material removal rate and taper angle of armor steel.

The material removal action succeed due to the mixing of pressurized water and coarse particles shearing action takes place on the workpiece. The most influencing parameter in the material removal rate is traverse speed. While the traverse speed is minimum the rate of mater removal is low while the traverse speed increases the material removal rate is increase is depend upon the water jet pressure and Standoff distance. The highest material removal rate (205.56mm^3/min) observed on Traverse

speed is 15mm/min and Pressure is 260Mpa lowest material removal rate (18.64mm^3/min) is observed on Traverse speed is 5mm/min and Pressure is 220Mpa.

The kerf angle is depended upon the jet traverse speed and water pressure previous literature are also concluded that. The increasing of kerf angle is directly propositional to the jet traverse speed and water pressure. When the traverse speed is 5 mm/min @ pressure 220, 240 and 260 and the SOD is 1mm it produces negative kerf angle due to close contact between the workpiece and the nozzle head continuous hitting of coarse particles bottom side is deviated. With increasing in jet traverse speed and standoff distance positive kerf angle are produced. The SOD process parameter significantly impacts the response, Ka. The variation in Ka is due to the hardness of the material. SOD and T should be kept at minimum. The lower Ka (0.651°) is obtained at SOD =1mm, T = 10 mm/min and P = 220 MPa.

In this study, Ra is initially low as Jp increases. But the surface roughness increase-es as the P increase further. It is an identity that increasing the JP (up to 240 MPa) re-duces the Ra. Minimizes the chances of plastic deformation and micro-cutting. In-creases in Jp and Jt will alter the roughness of the surface. It is due to the size and type. The P and its interaction do not affect the roughness of the character in this case. When P is in-creased, abrasive fragments is also increased along with their enhanced rate. Due to fragmentation, the size of impacting abrasive particles is reduced. Similarly, when P is increased, the kinetic energy of the water jet also increased, affecting the surface roughness. The Jt, second-order terms of P, and Jt are identified as significant process parameters for Ra, based on the experimental results. The standoff distance does not have any physical effect on the roughness of the surface, as previously stated in the literature. With a large SOD, more contact P is produced than with a small SOD. It makes a better machining surface Ra is predicted to be reduced by in-creasing Jt since the number of abrasive particles that are imposed on the workpiece gets reduced by increasing Jt.

Chapter 5: This chapter discusses the outcomes of AWJM process parameters on top kerf width, bottom kerf width, surface roughness and kerf angle of Armor steel. Semi-Empirical model was created using Buckingham's π theorem. The experimental results compare with semi empirical model and regression model. Also discusses the ANOVA and report the percentage contribution of each parameter on the response.

From the ANOVA results it is evident that Jt 85.38% had the greatest effect on MRR compared to the other two process parameters. At A*B 0.31%, A * C 0.03% and B*C 1.56%, the influence of the interaction terms is insignificant (0.31%, 0.03% and 1.56%, respectively). The impacts of every process parameters are obtained by maintaining performance parameter, one variable constant which is kept as remaining constant. It is observed that when Jt increases, the MRR increases. Abrasive waterjet particles in the waterjet stream erode high-strength materials like armor steel, resulting in material loss. Thus, increased kinetic energy increases erosion rates and material removal rates. The machining rate increases with a higher traverse speed, removing more material from the workpiece. In turn, the material removal rate is determined mainly by the speed of the traverse. The semi-empirical modeling findings were compared with the experimental data and a regression model. Figure. 3 illustrates that the semi-empirical modeling is more accurate and precise than the regression model. The percentage error variance between experimental and predicted values is less than 5%.

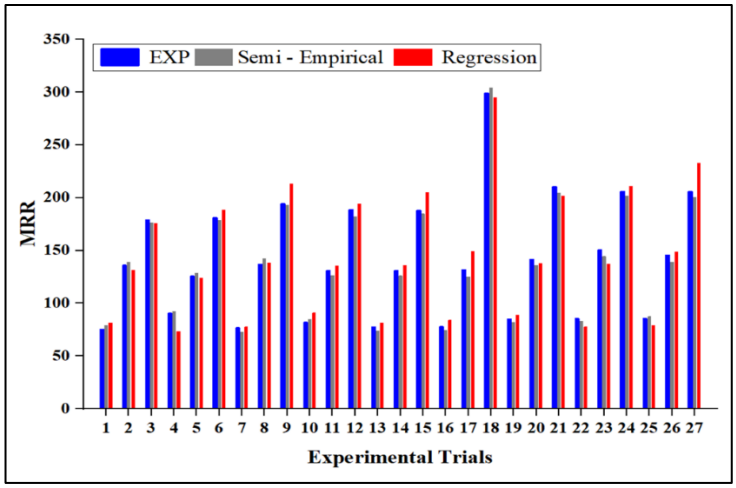

Figure 3. MRR comparison between experimental, semi-empirical and regression methods.

The ANOVA findings shows that jet traverse speed has the most significant effect on Ra compared to the other two machining factors. When increasing the SOD from 1mm to 2 mm, Ra gradually increases from 2.326 µm to 4.516 µm and after that decreases to 2.94 µm at 3 mm. Ra increases from 3.14 µm to 3.28 µm when P is increased from 220 MPa to 260 MPa. The roughness of the surface is directly related to the JT. From 2.85 to 3.58 µm, the Ra is directly proportional to JT. P increases the

particle's kinetic energy and substantially increases its MRR, while decreasing Ra. In this study, Ra is initially low as P increases. But the Ra increases as the P increase further. It is an identity that increasing the P (up to 240 MPa) reduces the Ra. Minimizes the chances of plastic deformation and micro-cutting. Increases in P and JT will alter the roughness of the surface. It is due to the size and type. The P and its interaction do not affect the roughness of the character in this case. When P is increased, abrasive fragments is also increased along with their enhanced rate. Due to fragmentation, the size of impacting abrasive particles is reduced. Similarly, when P is increased, the kinetic energy of the water jet also increased, affecting the Ra. The JT, second-order terms of P, and JT are identified as significant process parameters for Ra, based on the experimental results. The semi-empirical modeling is validated by evaluating it to Ra's experimental data and regression model. The variations for each observation number for semi-empirical, observed, and regression model Ra values are shown in Figure 4.

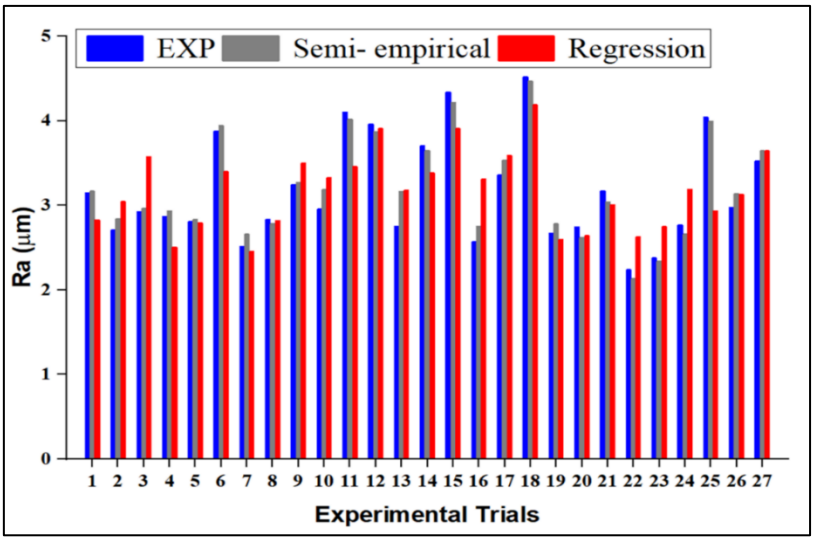

Figure 4. Comparison between experimental, semi-empirical and regression methods.

Ka initially decreases from 0.727 to 0.720 while the P gets varied. Then Ka increases exponentially to 0.746 for a further increase in P. There is a significant relationship among SOD, P, JT, and Ka. While JT increases, Ka decreases as shown in Figure 8 a. When JT increases from 5 mm/min to 10 mm/min; Ka increases from 0.752 ° to 0.722°; when the JT is increased to 15 mm/min, the taper angle has been reduced to 0.719 °. The variance in Ka is due to the hardness of the material. SOD and JT should be kept to a minimum. Ka decreases as the hydraulic P increases. This is because, kinetic energy is enlarged the velocity transfer of abrasives, resulting in a diminished

K_{bw}. The kinetic energy and cutting performance of the particles are enhanced with increased P. As P increased from 240 MPa to 260 MPa, the top kerf increased due to the increase in Ka. At the base of the workpiece, the waterjet kinetic energy decreases. It cannot remove the material efficiently and therefore creates a narrow K_{bw}, resulting in a decrease in Ka. A similar trend has been seen in Armor steel cutting. Ka increased with an increase in SOD. At high speeds, the jet will deviate. The jet increases as it exits the nozzle. The workpiece surface is now exposed to the bottom of the waterjet after the SOD gets raised. As the water jet diverges, it loses uniformity, which diminishes the cutting area seen in Ka immediately after that. Similarly, increasing Jt tends to increase Ka. When Jt value is low, the nozzle allows a high volume of abrasive particles to strike the workpiece. As a result, a larger volume of material is removed, resulting in a higher K_{tw}. At the same time, the waterjet penetrates thoroughly the workpiece, maintaining kinetic energy and efficiently cutting the bottom material. The kerf width variation reduces the taper angle. The correct taper is obtained at SOD (1mm), JT (10 mm/min), and P (220 MPa). The reverse taper is obtained at SOD (3 mm), JT (5 mm/min) and P (240 MPa). The findings of the semi-empirical model show a good connection between experimental and predicted values. Figure 5 shows that semi-empirical models outperformed regression models. The observed and anticipated values varied by less than 5%.

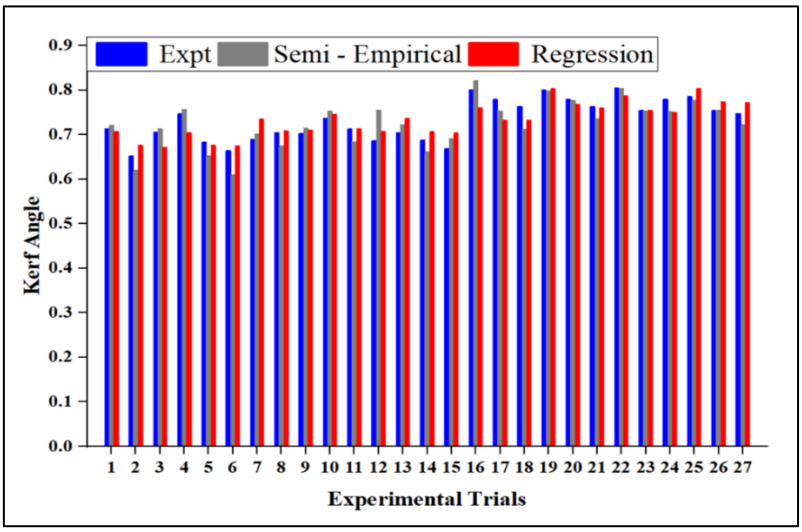

Figure 5. Comparison of Ka between experimental, semi-empirical and regression methods.

Chapter 6: In this chapter, Numerical modeling of kerf generation by using SPH-DEA-FEM approach. Numerical model created for waterjet material using SPH. Abrasive model createed by using DEA and the material model created by using Johnson-Cook model. Finally, the simulation model validity is verified through experiments.

After the AWJM cutting is completed, the sample is scanned and the top and bottom kerf widths are measured using image J software. The average value of the measurements is used as the records of the corresponding parameter, the top and bottom widths of the kerf in order to guarantee the quality of the cut profiles. The AWJM cutting process is simulated and then, it is compared with the experimental results at varying jet traverse speeds and jet water pressures. Initially, the mean velocity of water flow rate and the mean abrasive flow rate are first determined using the experimental water pressure as shown in equation 14 and 15. Secondly, in accordance with the laws of motion relativity, the simulation model is modified such that the workpiece is moved in reverse direction of traverse speed, and abrasive waterjet is permanently placed. The cutting depths are finally determined for various levels of traverse speed and water pressure as shown in Figure 6.

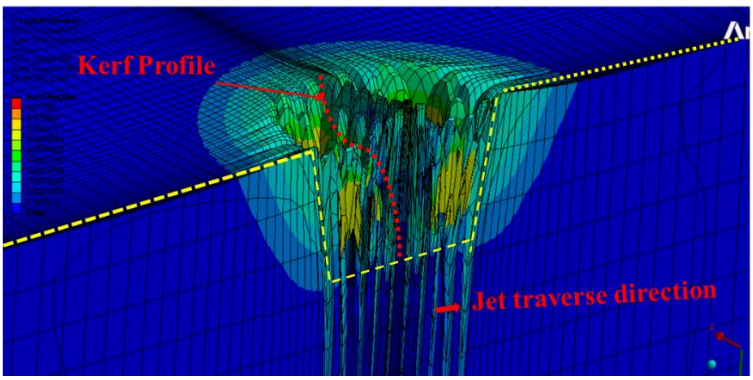

Figure 6. Center cross-section Y-Y view of the FEM workpiece output after being exposed to the effects of an abrasive waterjet

A wider top kerf width is observed when SOD is increased from 1-3 mm. The distance between where the water stream comes out of the nozzle and where it hits the specimen is the standoff distance. At a greater standoff distance, the water jet gets wider and deviates from the neutral axis. The water jet expansion and divergence together cause the abrasive particles to lose the velocity and the kinetic energy. A wider kerf is

produced at the top, due to the impact of the enlarged jet, while the bottom kerf is narrowed, since the jet's velocity is reduced. With an error of 32% predicated at the top kerf width, the experimental data and the simulation results are in agreement.

As T is increased from 5-15 mm/min, an inverse relationship was observed for the kerf widths. Due to the lack of exposure time, abrasive particles have lower chance of making a strong impact on the specimen, when the jet transverse speed is increased. The predicted top kerf width error is around 40%. The validity of simulation findings is used to process the control and operational parameter optimization and it is later confirmed by the reasonable agreements.

Top kerf width in AWJM varies with jet pressure. When the jet pressure increases, the water waves move faster. The abrasive particles combined kinetic energy is increased by their high velocity impacts. The water stream impacts the specimen more severely and widens the top kerf, due to turbulence, inter-particle collisions, and increased kinetic energy. Errors of less than 26% have been found between the simulated and the experimental AWJM cutting at top kerf width. Thus, it can be concluded that the simulated results match well with the experimental results.

For improved control of the AWJM machining process, it is crucial to examine the kerf formation process and its geometric properties. Currently, there is no direct means for observing the evolution process without using a dependable AWJM simulation model. Figure 9 depicts the process of kerf creation produced by the high velocity abrasive particle impacts on the target surface. The top width of the cutting is observed to rise through time, but the profile remains stable till the jet passes. The simulations have created a typical AWJM eroded surface, which is seen in Figure 10. It can be observed that the pressure distribution in various impacted locations is not uniform. Pressure is the lowest in the center square and it increases, when it moves outside. Along these lines, the rate of material removal also confirms with this pattern. The material is removed more quickly from the jet's outer edges, but it is not effectively removed from the jet center. The trajectories of water flow rate and abrasive particles flow rate in Figure 10a provide an explanation for this disparity. Once the jet beam first strikes the workpiece, its perimeter expands quicker than releasing wave produced by the hydraulic shock. As a result, an internal shock waveis developed inside the waterjet. As the shock wave grows, the abrasive particles enter into the jet and it causes the shock front to eventually achieve a quasi-steady state as well as starts removing material. The middle section of the waterjet is defined as a pressure stagnation zone. In addition, the

pressure of the abrasive water jet is the lowest in the centre and the highest in the periphery, when it hits the surfaces of the target, resulting in a disc-shaped stress dispersion. Also, the material has also piled around the edges of the simulated kerfs and it is shown in Figure 7.

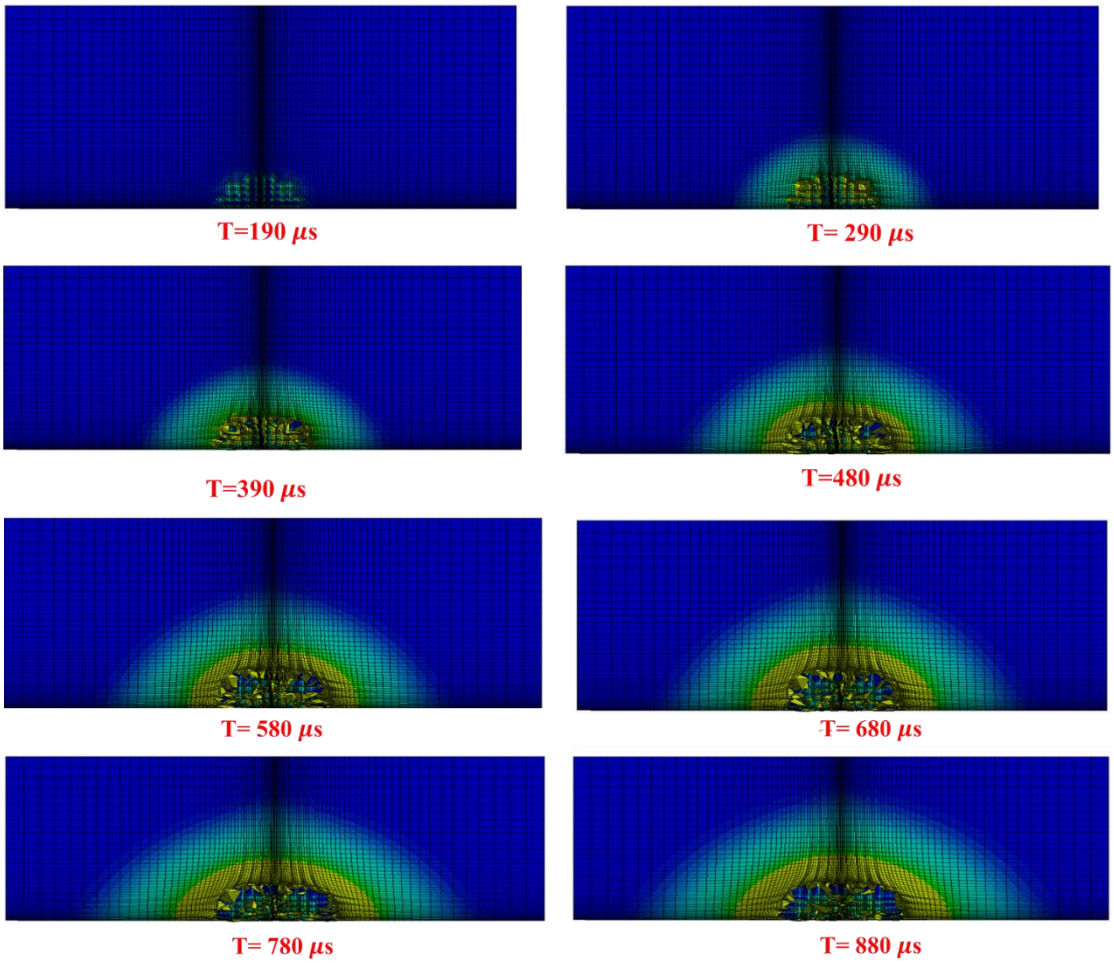

Figure 7. AWJM Simulation results at different time periods

Chapter 7: In this chapter the conclusion of the research work and the scope for the future work are presented based on the results and discussion.

- The increase in traverse speed and water jet pressure will lead to increase in kerf width.
- The material removal rate depends upon the jet traverse speed and water jet pressure when the jet traverse speed is minimum and the pressure also minimum material removal rate is reduced increase of water jet pressure and jet traverse speed material removal rate is more.
- At low Jet traverse speed, moderate jet pressure with, machining of armor

steel can give good surface finish.

- Confirmation experiments show that the residuals between predicted and experimental values are less than 5%. The values of the semi-empirical modeling and regression models are compared with the experimental values. For MRR, Ra, and Ka, the semi-empirical model is proved to be more accurate than the regression model, to predict the variables relationships.
- The use of the analysis of variance approach in combination with the dimensional analysis reduced the number of insignificant variables and resulted in simpler models for MRR, Ra and Ka.
- The maximum MRR is obtained at SOD = 2mm, JT = 15mm/min and P = 260MPa. Improved MRR is achieved due to the greater kinetic energy of the jet produced by this combination. These findings demonstrate that a higher surface finish is attained with a higher SOD = 3mm and lower JT = 5mm/min. This allows for a more uniform MRR, which results in a lower roughness. Ra is determined to be 2.23 µm.
- The SOD process parameter significantly impacts the response, Ka. The variation in Ka is due to the hardness of the material. SOD and JT should be kept at minimum. The lower Ka (0.651°) is obtained at SOD =1mm, JT = 10 mm/min and P = 220 MPa.
- Microstructural analysis of machined surfaces reveals three regions: top, middle, and bottom. In the top region, smooth surfaces are obtained, and in the middle region, fewer voids are present, and less ploughing is identified at the bottom.
- In future the research may be extended on comparison of experimental results with numerical modelling studies. The results obtained can be applied in battel field vehicle applications.
- Automated particle and water flow generation are used in the model. This makes it possible to simulate AWJM for long period of time on thick plates and it greatly improves the efficiency.
- Using the experimental data, the model has been proved to provide accurate predictions of the cutting performance and its potential utility is suggested in process control and operating parameter optimization.

- The pressure stagnation region formed in the centre of the waterjet prevents the erosion of the material in the centre of the affected region. Particles hitting the kerf walls cause the material to pile up toward the kerf boundaries.
- Experimental tests produced hydraulic shock waves, vibrations, lag of abrasive flow etc. But during the simulation, a controlled environment without any energy losses was defined.
- Future research extends to consider the environmental and other desirable machine factors to reduce the simulation errors.

FUTURE WORK

- The process parameters like varying the impact angle of jet, type of abrasive particles and size of the abrasive can be varied and a detail study can be done.
- The proposed work can further be optimized through metaheuristic techniques such as Artificial Neural Network, Cuckoo algorithm, Particle swam optimization, Simulated annealing etc., on reducing the surface roughness and kerf angle.
- Cryogenic assisted cutting can also be performed.

REFERENCES

1. B.B.Singh, G.Sukumar, K.Sivakumar, V.Madhu, R.A.Kumar, comparative study on the ballistic performance of high nitrogen steel and rolled homogeneous armour steel against 7.62 mm ball and 12.7 mm armour piercing projectiles. *Materials Today: Proceedings*, **41** (5) (2021) 1188-1194.
2. R.Bobbili, V.Madhu, A.K.Gogia, Effect of Wire-EDM Machining Parameters on Surface Roughness and Material Removal Rate of High Strength Armor Steel. *Materials and Manufacturing Processes*, **28** (4) (2013) 364–368.
3. M. Balakrishnan, V.Balasubramanian, G.Madhusudhan Reddy, Microstructural analysis on ballistic tested armour steel joints fabricated using low hydrogen ferritic consumables for capping pass. *Key Eng. Mater*, **812** (2019) 1–8.
4. Atapek, S. Karagoz, Ballistic impact behaviour of a tempered bainitic steel against 7.62 mm armour piercing projectile. *Defence Science Journal*, **61** (2011) 81–87.
5. B.Ilhak, F.Güner, Failure Analysis of Boron Carbide-Reinforced Rolled Homogeneous Armour Against Kinetic Energy Ammunition. *Trans Indian Inst Met*, **75** (2022) 1831–1841.
6. B.B.Singh, G.Sukumar, P.P.Senthil, P.K.Jena, P.R.S.Reddy, Future Armour Materials and Technologies for Combat Platforms Future Armour Materials and Technologies for Combat Platforms. *Defence Science Journal*, **64 (4)** (2017) 412-419.
7. D. Arola, M.Ramulu, Material removal in abrasive waterjet machining of metals. *Surface integrity and texture*, **210** (1-2) (1997) 50-58.
8. S.Ramakrishnan Investigating the effects of abrasive water jet machining parameters on surface integrity, chemical state in machining of Ti-6Al-4V. *Materials Today Communications*, **31**, (2022) 103480.
9. Hashish, M. A Modeling Study of Metal Cutting With Abrasive Waterjets, *J. Eng. Mater. Technol*, **106** (1) (1984) 88-100. K.
10. S.Palaniyappan, A.Veiravan, R.Kaliyamoorthy, V.Kumar, Sustainable solution to low-cost alternative abrasive from electric ceramic insulator waste for use in abrasive water jet machining. *Int J Adv Manuf Technol*, **120**, (2022) 5243–5257.
11. Kulekci, M.K. Processes and apparatus developments in industrial waterjet applications. *Int. J. Mach. Tools Manuf*, **42** (12) (2002) 1297–1306.

12. Lenihan, D, Ronan, W, O'Donoghue, P.E. and Leen, S.B, A review of the integrity of metallic vehicle armour to projectile attack. *Proceedings of the Institution of Mechanical Engineers, Part L: Journal of Materials: Design and Applications*, **233** (1) (2019) 73-94.
13. K.Senthil, K. and M.A.Iqbal, Prediction of superior target layer configuration of armour steel, mild steel and aluminium 7075-T651 alloy against 7.62 AP projectile. *In Structures*, **29** (2021) 2106-2119.
14. A. Banerjee, S. Dhar, S. Acharyya, D. Datta and N. Nayak, Determination of Johnson cook material and failure model constants and numerical modelling of Charpy impact test of armour steel. *Materials Science & Engineering A*, **640** (2015) 200-209.
15. M.A. Iqbal, K. Senthil, P.Sharma, and N.K. Gupta, An investigation of the constitutive behavior of Armox 500T steel and armor piercing incendiary projectile material. *International Journal of Impact Engineering*, **96** (2016) 146-164.
16. B.B. Singh, G. Sukumar, P.P. Rao, K.S. Kumar, V. Madhu, and R.A.Kumar, Superior ballistic performance of high-nitrogen steels against deformable and non-deformable projectiles. *Materials Science and Engineering*, **751** (2019) 115-127.
17. O.G GHIORGHE, C.SCHNAKOVSZKY, E.HERGHELEGIU, & C.TAMPU, (2022). Study On The Influence Of Wedm Processing Regimes On The Quality Of Armor Steel. *Journal of Engineering Studies and Research*, **28** (3) (2022) 49-55.
18. R.Bobbili, V.Madhu & A. K Gogia Effect of Wire-EDM Machining Parameters on Surface Roughness and Material Removal Rate of High Strength Armor Steel. *Materials and Manufacturing Processes*, **28** (4) (2013) 364-368.
19. T.A.El-Taweel, and A.R.El-Desouky, 2011. Effect of edm assisted by magnetic field on surface integrity of armoured steel. *ERJ. Engineering Research Journal*, **34** (1) (2011) 57-69.
20. J.Wang, Depth of cut models for multipass abrasive waterjet cutting of alumina ceramics with nozzle oscillation. *Front. Mech. Eng. China*, **5** (2010) 19–32.

21. Y.Yuan, , J.Chen, , H.Gao, et al. An investigation into the abrasive waterjet milling circular pocket on titanium alloy. *Int J Adv Manuf Techno,l* **107** (2020) 4503–4515.
22. D.K.Shanmugam, S.H.Masood, An investigation on kerf characteristics in abrasive waterjet cutting of layered composites. *Journal of Materials Processing Technology*, **209** (8) (2009) 3887–3893.
23. D.Singh, R.S.Shukla, Integration of quality characteristics models as a software-based graphical interface for machining of AA6351 aluminum alloy using abrasive water jet process. *J. Brazilian Soc. Mech. Sci. Eng*, **42** (2020) 330.
24. R.Pahuja, M.Ramulu, Abrasive water jet machining of Titanium (Ti6Al4V)–CFRP stacks – A semi-analytical modeling approach in the prediction of kerf geometry. *J. Manuf. Process*, **39** (2019) 327–337.
25. V.Mohankumar, M.Kanthababu,; Velayudham, A. Abrasive waterjet cutting of boron carbide particles reinforced Al 6063 MMCs – A semi empirical modeling approach in the prediction of kerf angle. *Measurement*, **181** (2021) 109492.
26. D. Kumar, S. Gururaja, Abrasive waterjet machining of Ti/CFRP/Ti laminate and multi-objective optimization of the process parameters using response surface methodology, J. Compos. Mater, **54** (13) (2020) 1741–1759.
27. P. Thamizhvalavan, S. Arivazhagan, N. Yuvaraj, B. Ramesh, Machinability study of abrasive aqua jet parameters on hybrid metal matrix composite, *Mater. Manuf. Process*. **00** 2018 1–24.
28. D. Singh, R.S. Shukla, Investigation of kerf characteristics in abrasive water jet machining of inconel 600 using response surface methodology, *Def. Sci. J*, **70** (2020) 313–322.
29. A. Shanmugam, K. Krishnamurthy, T. Mohanraj, Experimental study of surface roughness and taper angle in abrasive water jet machining of 7075 aluminum composite using response surface methodology, *Surf. Rev. Lett*, **27** (2020) 1–9.
30. Jianming, W., Na, G. & Wenjun, G. Abrasive waterjet machining simulation by SPH method. *Int J Adv Manuf Technol*, **50** (2010) 227–234.
31. S. Anwar, D.A. Axinte, A.A. Becker, Finite element modelling of overlapping abrasive waterjet milled footprints, *Wear*, **303** (2013) 426–436.

32. J.N. Nyaboro, H. El-Hofy, M.A. Ahmed, M. El-Hofy, Numerical and experimental characterization of kerf formation in abrasive waterjet machining, *ASME Int. Mech. Eng. Congr. Expo. Proc*, **2** (2018) 1–10.
33. G.Wenjun, W.Jianming, & G.Na, Numerical simulation for abrasive water jet machining based on ALE algorithm. *Int J Adv Manuf Technol*, **53** (2011) 247–253.
34. P. Lozano, D Torrubia, A. Axinte, J. Billingham, Stochastic modelling of abrasive waterjet footprints using finite element analysis, *Int. J. Mach. Tools Manuf*, **95** (2015) 39–51.

LIST OF PUBLICATIONS

1. S. Rammohan, S. Thirumalai Kumaran. M. Uthayakumar, *et al.* Application of TOPSIS Optimization in Abrasive Water Jet Machining of Military Grade Armor Steel. *Hum Factors Mech Eng Def Saf.* **5** (2021) 3.
2. Rammohan, Soundarapandian, Sundaresan Thirumalai Kumaran, Marimuthu Uthayakumar, Kinga Korniejenko, Marek Nykiel, and Arumugam Velayutham. *"Prediction of Abrasive Waterjet Machining Parameters of Military-Grade Armor Steel by Semi-Empirical and Regression Models." Materials* **1 5** (12) (2022) 4368.
3. S. Rammohan, S. Thirumalai Kumaran, M. Uthayakumar and A. Velayudham "*Numerical modelling of kerf generation in abrasive waterjet machining of military grade armor steel*", *Hum Factors Mech Eng Def Saf.* **5** (2023) 3.